Vol 16 No 4, April 2007
1009-1963/2007/16(04)/1042-05
Chinese Physics
© 2007 Chin. Phys. Soc.
and IOP Publishing Ltd

Atomic coherence in nondegenerate four-wave mixing*

Zuo Zhan-Chun(左战春)[a], Sun Jiang(孙 江)[b], Liu Xia(刘 霞)[a],
Mi Xin(米 辛)[a], Yu Zu-He(俞祖和)[a], Jiang Qian(姜 谦)[a],
Fu Pan-Ming(傅盘铭)[a], and Wu Ling-An(吴令安)[a]

[a] *Laboratory of Optical Physics, Beijing National Laboratory for Condensed Matter Physics, Institute of Physics, Chinese Academy of Sciences, Beijing* 100080, *China*

[b] *Department of Physics, Hebei University, Baoding* 071002, *China*

(Received 28 June 2006; revised manuscript received 18 August 2006)

Two-photon resonant nondegenerate four-wave mixing (NFWM) with the addition of a coupling field in Ba atomic vapour has been studied. We find that coherence of the atomic level transitions leads to suppression of the NFWM signal, giving rise to a dip with a linewidth that is linearly proportional to the intensity of the coupling field.

Keywords: nondegenerate four-wave mixing, electromagnetically induced transparency
PACC: 4256M, 4250V

1. Introduction

The influence of atomic coherence in nonlinear optics has aroused much interest in recent years.[1−3] For example, electromagnetically induced transparency (EIT) can not only give rise to the transparent transmission of stimulated radiation but also increase the conversion efficiency without the need for strict phase matching conditions. Agarwal and Harshwardhan[4] showed that in a ladder-type four-level system, two-photon excitation may be selectively suppressed or enhanced by coupling the intermediate state to a higher-excited state and creating interference among the dressed-state transitions. Suppression of two-photon absorption in Na and cold Rb atoms was reported by Gao *et al*[5] and Yan *et al*,[6] respectively. There has been much work on saturation in EIT. Shakhmuratov *et al*[7] proposed theoretically that the width of the transparency window could be made very wide by saturation broadening. Krmpot *et al*[8] experimentally found that narrow EIT was possible only when a probe was tuned to a closed transition and optical pumping and saturation were dominant mechanisms.

Linewidth broadening is caused by several factors. The natural linewidth is due to spontaneous radiation from the atoms, whilst Doppler broadening and collision broadening (pressure broadening) are caused, respectively, by the motion of atoms and the collisions between particles or between particles and wall. There is also another type of broadening which increases with increasing radiation intensity, and is known as power-broadening (saturation broadening). The change of linewidth can indicate many factors. For example, Doppler-broadening is related to the hole-burning effect and the Lamb dip. According to the simulated line shape and linewidth we can deduce many properties like the transverse relaxation rate and transition dipole moment, thus spectral linewidth is an important characteristic in spectroscopy. Javan *et al*[9] showed that for a relatively weak driving field the EIT linewidth is proportional to the square root of the intensity and is independent of the Doppler width. In the limit of high intensity they recovered the usual power-broadening case where the EIT linewidth is proportional to the intensity and inversely proportional to the Doppler width. Mikhailov *et al*[10] reported transmission linewidths for a weak anti-Stokes component and generated a Stokes component during resonant four-wave mixing in atomic Rb vapour. Agarwal showed in his paper[4] on inhibition and enhancement of two-photon absorption that, by using a control laser to couple the intermediate state with some other state, the medium can be made transparent instead of two-photon absorbing. It has also been shown that field-induced quantum interference and the consequent transparency effects can be exploited to enhance nonlinear optical cross sections, decrease

*Project supported by the National Natural Science foundation of China (Grant Nos 10174096 and 10374113) and the National Program for Basic Research in China (Grant No 001CB309301).
†E-mail: wula@aphy.iphy.ac.cn

the switching threshold of optical bistability, realize lasing without inversion, and increase the refractive index. These ideas have also been used for quenching spontaneous emission noise.

Recently, in our experiments on quantum interference and two-photon resonant nondegenerate four-wave mixing (NFWM) in Ba atomic vapour[11−13] we observed suppression and enhancement of the signal as a result of the atomic coherence between the Rydberg 6s19d state and autoionizing 6p19d state. In this paper we report further atomic coherence effects in a similar NFWM setup (see Fig 1(a)) for the Ba system, wherein resonant NFWM signal dips appear due to the strong coherence induced by a coupling field. Suppression of the NFWM signal occurs because of the coherence between the level transitions induced by the coupling field, and we find that the width of the dip is proportional to the intensity of the field. Based on this type of resonant excitation in a cascade four-level system, highly excited atomic states can be studied with high sensitivity. The technique is Doppler-free when the incident lasers have narrow bandwidths. Most importantly, our method can measure transitions between two highly excited atomic states which have long radiative lifetimes so that a direct detection of the fluorescence is difficult. It is thus an effective spectroscopic tool for studying atoms in a highly excited state or highly angular momentum state.

2. Basic theory

Let us consider a four-level system in the cascade configuration (Fig.1(a)), where states $|0\rangle$ and $|1\rangle$, $|1\rangle$ and $|2\rangle$ and $|2\rangle$ and $|3\rangle$ are coupled by dipolar transitions with resonant frequencies Ω_1, Ω_2 and Ω_3 and dipole moment matrix elements μ_1, μ_2 and μ_3, respectively. We first consider two-photon resonant NFWM in the $|0\rangle$-$|1\rangle$-$|2\rangle$ three-level cascade system with the geometry shown in Fig.1(b), Here beams 2 and $2'$ have the same frequency ω_2 and a small angle between them; beam 1 with frequency ω_1 propagates in the opposite direction to beam 2. We assume that $\omega_1 \simeq \Omega_1$ and $\omega_2 \simeq \Omega_2$, so that ω_1 and ω_2 drive the transitions from $|0\rangle$ to $|1\rangle$ and $|1\rangle$ to $|2\rangle$, respectively. In this case, the simultaneous interactions of atoms with beams 1 and 2 will induce atomic coherence between states $|0\rangle$ and $|2\rangle$ through two-photon excitation. This coherence is then probed by beam $2'$, and as a result an NFWM signal beam of frequency ω_1 is generated, along a direction approximately opposite to beam $2'$. To study the coherence in this system, we apply a coupling laser (beam 3) of frequency ω_3 ($\simeq \Omega_3$), which can propagate either along or opposite to the direction of beam 2, to drive the transition from $|2\rangle$ to $|3\rangle$. As a result, in the bare-state picture, atomic coherence is induced between states $|0\rangle$ and $|3\rangle$.

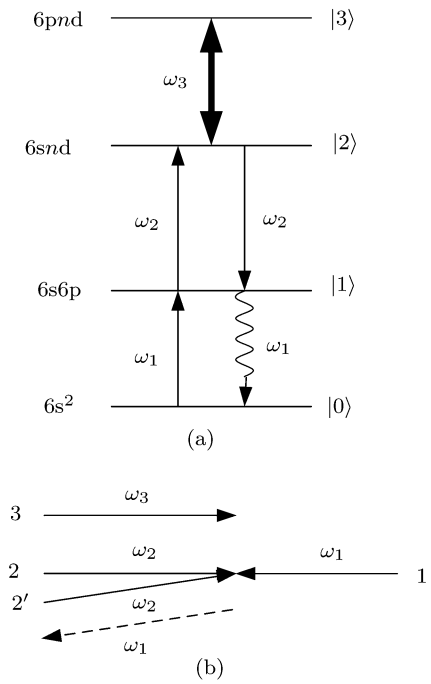


Fig.1. Energy-level diagram for two-photon resonant NFWM with a coupling field. (b) Schematic of two-photon resonant NFWM with a coupling field.

Let Δ_s' represent the various detunings: $\Delta_1 = \Omega_1 - \omega_1$, $\Delta_2 = \Omega_2 - \omega_2$, $\Delta_3 = \Omega_3 - \omega_3$. After a canonical transformation the effective Hamiltonian is expressed as

$$H = \hbar\Delta_1|1\rangle\langle 1| + \hbar(\Delta_1+\Delta_2)|2\rangle\langle 2| + \hbar(\Delta_1+\Delta_2+\Delta_3)|3\rangle\langle 3| - (\mu_1 E_1|0\rangle\langle 1| + \mu_2 E_2|1\rangle\langle 2| + \mu_3 E_3|2\rangle\langle 3| + \text{H.c.}). \quad (1)$$

Here, $E_1 = \varepsilon_1 e^{i\boldsymbol{k}_1\cdot\boldsymbol{r}}$, $E_2 = \varepsilon_2 e^{i\boldsymbol{k}_2\cdot\boldsymbol{r}} + \varepsilon_2' e^{i\boldsymbol{k}_2'\cdot\boldsymbol{r}}$ and $E_3 = \varepsilon_3 e^{i\boldsymbol{k}_3\cdot\boldsymbol{r}}$ are the complex incident laser fields with frequencies ω_1, ω_2 and ω_3, respectively; while $\boldsymbol{k}_1$, $\boldsymbol{k}_2$, $\boldsymbol{k}_2'$ and $\boldsymbol{k}_3$ are the wave vectors of beams 1, 2, $2'$ and 3, respectively. The nonlinear polarization $|P_T|$ responsible for the two-photon resonant NFWM signal is proportional to the off-diagonal density matrix element ρ_{10}. We will assume, as usual, that the field amplitudes ε_1, ε_2 and ε_2' are weak, whereas the coupling field ε_3 can be of arbitrary magnitude. Thus ρ_{10} needs to be calculated to the order of ε_1 ε_2 ε_2',

but to all orders in ε_3. This can be done using density matrix equations with relaxation terms properly included

$$\frac{\mathrm{d}\rho}{\mathrm{d}t} = -\frac{\mathrm{i}}{\hbar}[H,\rho] + \left(\frac{\mathrm{d}\rho}{\mathrm{d}t}\right)_{\mathrm{relax}}. \tag{2}$$

We obtain

$$\rho_{10}(\boldsymbol{r}) = -\mathrm{i}\frac{G_1 G_2 (G_2')^* [\mathrm{i}(\Delta_1+\Delta_2+\Delta_3)+\Gamma_{30}]\exp[i(\boldsymbol{k}_1+\boldsymbol{k}_2-\boldsymbol{k}_2')\cdot\boldsymbol{r}]}{(\mathrm{i}\Delta_1+\Gamma_{10})^2\{[\mathrm{i}(\Delta_1+\Delta_2)+\Gamma_{20}][\mathrm{i}(\Delta_1+\Delta_2+\Delta_3)+\Gamma_{30}]+|G_3|^2\}}, \tag{3}$$

where Γ_{n0} is the transverse relaxation rate between states $|n\rangle$ and $|0\rangle$ and $n = 1, 2$ or 3; the G's denote the coupling coefficients $G_1 = \mu_1\varepsilon_1/\hbar$, $G_2 = \mu_2\varepsilon_2/\hbar$, $G_2' = \mu_2\varepsilon_2'/\hbar$ and $G_3 = \mu_3\varepsilon_3/\hbar$. According to Eq.(3), the NFWM phase conjugate signal propagates along the direction $\boldsymbol{k}_1 + \boldsymbol{k}_2 - \boldsymbol{k}_2'$. The signal intensity is proportional to $|P_{\mathrm{T}}|$, which is independent of the direction of the coupling field $\boldsymbol{k}_3$. In other words, the application of a coupling field does not affect the phase matching condition of the two-photon resonant NFWM. We study the change of the signal linewidth when Δ_3 is scanned. If $\Delta_1 + \Delta_2 = 0$, then

$$I_{\max} = \frac{|G_1 G_2 G_2'|^2}{(\Delta_1^2+\Gamma_{10}^2)^2\Gamma_{20}^2}, \tag{4}$$

$$I_{\min} = \frac{|G_1 G_2 G_2'|^2\Gamma_{30}^2}{(\Delta_1^2+\Gamma_{10}^2)^2(\Gamma_{20}\Gamma_{30}+|G_3|^2)^2}. \tag{5}$$

The linewidth is $\delta\omega = 2\Gamma_{30}' + 2G_3^2/\Gamma_{20}'$, which will increase with the intensity of laser ω_3. The atomic transition line shape will change with the relevant particle population through stimulated radiation or absorption, so the field intensity induces linewidth broadening, i.e., power broadening (or saturated broadening). If we take states $|2\rangle$ and $|3\rangle$ as a two-level atom system with a coupling field, then from the power broadening equation: $\delta\omega' = (\Gamma_{30}'^2 + G_3^2)^{1/2}$, we find that the linewidth of the NFWM signal is wider than that due to power broadening alone.

3. Experimental Results

The experimental setup is shown in Fig.2. Barium vapour is contained in a stainless-steel heat-pipe oven with argon as buffer gas. The oven temperature is 660^o C and the pressure 133.32 Pa. Here the ground state $6s^2$ ($|0\rangle$), intermediate state 6s6p ($|1\rangle$), Rydberg state 6snd ($|2\rangle$) and the doubly excited autoionizing Rydberg state 6pnd ($|3\rangle$) form a folded four-level system (see Fig.1(a)). Three dye lasers L1, L2 and L3, which are pumped by the second harmonic of a Quanta-Ray Nd:YAG laser, have a linewidth of 0.007 nm, pulsewidth 5 ns and repetition rate 10 Hz. All the incident beams are linearly polarized in the vertical polarized direction and are focused to a spot approximately 2.0 mm in diameter at the oven. Laser L1 is tuned to 553.5 nm, the wavelength of the $6s^2\ {}^1S_0$–$6s6p\ {}^1P_1$ transition. The beam from laser L2 is split at the beam splitter BS1 into beams 2 and 2′, which then intersect in the Ba vapour at a small angle of 0.5° to drive the transition from $6s6p\ {}^1P_1$ to $6sn\mathrm{d}\ {}^1D_2$. Laser L3 is scanned in the vicinity of the $6s_{1/2}$–$6p_{3/2}$ resonance lines of the Ba^+ ion ($\lambda_3 \sim 455$ nm) to reach the $6p_{3/2}n$d autoionizing states. The phase conjugate signal beam passes through beam splitter BS3, which transmits 50% at 553.5 nm, and is detected at the photodiode PD. The mirrors M are all high reflectors. In the experiment, the single pulse energies of beams 1 and 2 are $< 1\mu$J and 0.06mJ, respectively, while that of laser L3 is about 0.04mJ.

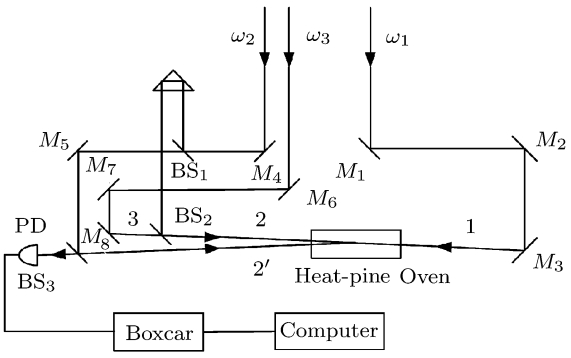


Fig.2. Experimental setup. BS': beam splitters; M': mirrors; PD: photodiode.

We first obtain the two-photon resonant NFWM spectrum by fixing ω_1 and scanning ω_2 over the whole tunable range of the second dye laser L2, which shows the Rydberg series of Ba. To avoid strong absorption at the resonant frequency of the transition from $6s^2$

$^1S_0$ to 6s6p $^1P_1$, the wavelength of L1 is detuned from exact resonance by 0.06 nm. We then set the wavelength of L2 at $\lambda_2 \sim 426.8$ nm to excite the Rydberg state 6s17d $^1D_2$, and scan ω_3 in the vicinity of the $6s_{1/2}$–$6p_{3/2}$ resonance lines of the Ba^+ ion. Figures 3(a), 3(b) and 3(c) show the NFWM signal intensity as a function of Δ_3 at exact two-photon resonance, i.e. $\Delta_1 + \Delta_2 = 0$ for different coupling field intensities. As can be seen, the signal intensity is suppressed when the frequency of the coupling laser L3 is scanned across the resonant frequency of the 6s17d $^1D_2$–$6p_{3/2}$17d transition. This is mainly caused by the interaction between the coupling field and four-wave mixing.

In our experiments the contribution from the Doppler effect to the linewidth of the dip in Fig.3(a) is only 0.05 cm^{-1}, so it can be neglected in our data analysis. On the other hand, the influence of the laser linewidths has to be considered. According to Ref.[14] the transverse relaxation rates Γ_{n0} in Eq.(3) should be replaced by $\Gamma'_{10} = \Gamma_{10} + \alpha_1$, $\Gamma'_{20} = \Gamma_{20} + \alpha_1 + \alpha_2$ and $\Gamma'_{30} = \Gamma_{30} + \alpha_1 + \alpha_2 + \alpha_3$, where α_1, α_2 and α_3 are the linewidths of lasers L1, L2 and L3, respectively. First, through fitting of the two-photon resonant NFWM spectrum, we obtain $\Gamma'_{20} = 0.7$ cm^{-1}. This value is mainly due to the laser linewidths because the lifetime of the Rydberg state 6s17d $^1D_2$ is of the order of μs. We then use Eq.(3) to fit the Δ_3-dependence spectra in Figs.3(a), 3(b) and 3(c). The solid curve is the theoretical curve with the following parameters: $|G_3|$ = 1.6 cm^{-1}, 2.0cm^{-1}, 3.4cm^{-1}, $\Delta_1 + \Delta_2 = 0$ cm^{-1}, $\Gamma'_{20} = 0.7$ cm^{-1}, and $\Gamma'_{30} = 20$ cm^{-1}. Here the transverse relaxation rate between $|0\rangle$ and $|3\rangle$ is dominated by the autoionization rate of the state $6p_{3/2}$17d. It is worth mentioning that although lasers of pulse-width $\tau_p = 5$ ns are used in our experiment, since $\Gamma'_{n0}\tau_p \gg 1$, the steady state solutions are valid for analysing our experimental results.

The dependence of the resonance dip linewidth on the intensity I_3 of the coupling field is shown in Fig.3(d), where the dots are experimental data and the solid line is the theoretical simulated curve $y = 40 + 32x$. We can see that the error is 5%, and that the dip linewidth broadens linearly with the increase of the field intensity. From the equation $\delta\omega = 2\Gamma'_{30} + 2G_3^2/\Gamma'_{20}$, we see that the linewidth $\delta\omega$ is mainly dependent on Γ'_{30} but also varies with $|G_3|^2$, which is proportional to the coupling field intensity I_3. Hence as the intensity I_3 increases, the dip linewidth broadens and, moreover, small dips become evident on both sides, as can be seen in Figs.3(b) and 3(c).

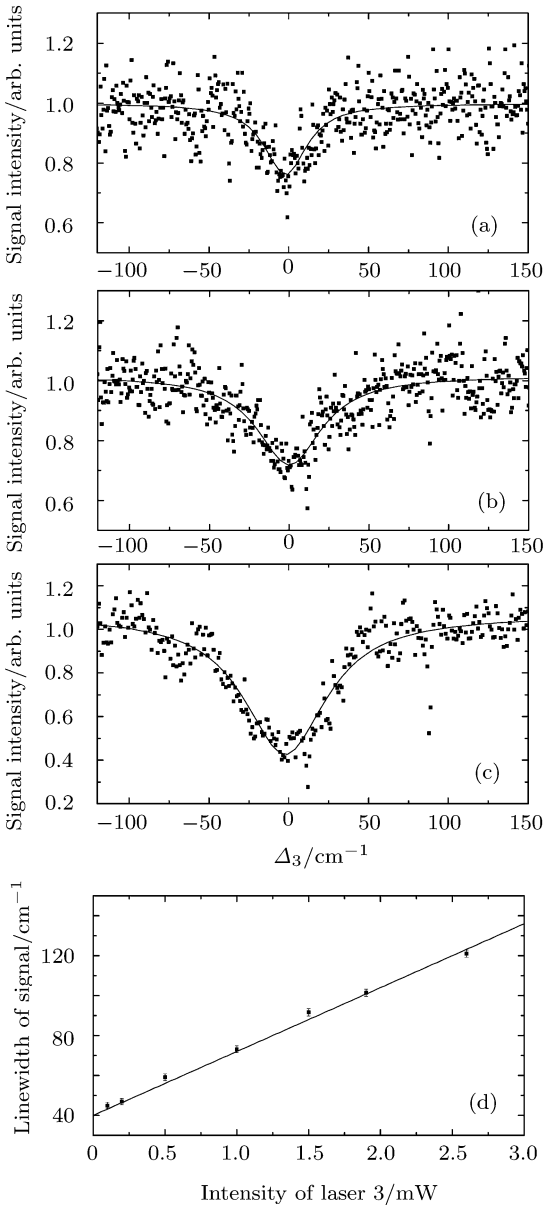


Fig.3. NFWM signal intensity as a function of Δ_3 at exact two-photon resonance with (a) I_3 = 0.2 mW, (b) I_3 = 0.4 mW, (c) I_3 = 1.0 mW, (d) dip linewidth as a function of the intensity of laser L3.

To study the origin of these small dips we perform a four-wave mixing experiment with beam 1 of frequency ω_1 but with beam 2 replaced by beam 3 of frequency ω_3. The NFWM signal obtained while scanning ω_3 is shown in Fig.4(a) as the bottom dotted curve. The top curve is the expanded spectrum of the NFWM signal in Fig.3(c) with ω_3 as the coupling field. We see that there are small dips which correspond to the peaks in four-wave mixing signal with frequencies ω_1 and ω_3 for transitions between 6s6p and 6sn'd or 6sn's, where n' is the principal quantum number of one of the two outer electrons. This can be

understood by referring to Fig.4(b) where the coupling beam can stimulate not only the 6snd ($|2\rangle$)–6pnd ($|3\rangle$) transition to induce atomic coherence between $|3\rangle$ and $|0\rangle$ but also other 6s6p ($|1\rangle$)–6sn'd ($|2'\rangle$) transitions to induce atomic coherence between $|2'\rangle$ and $|0\rangle$ resulting in suppression of the NFWM signal. Because 6s6p is the autoionizing state, the dip is wider than those for the 6snd and 6sn'd Rydberg states.

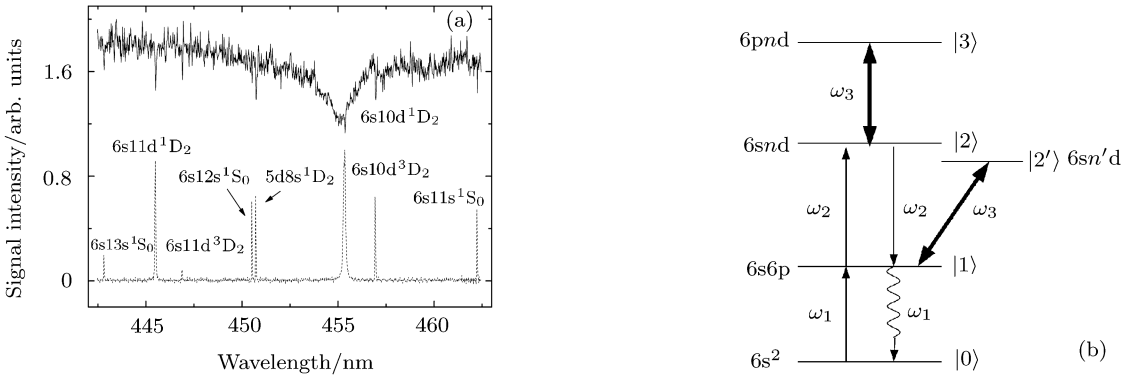


Fig.4. (a) NFWM spectrum with coupling field (top curve) compared with the NFWM signal obtained with beam 3 (ω_3) substituted for former beam 2 (ω_2) (bottom curve), as λ_3 is scanned. (b) Energy level diagram illustrating (a).

4. Conclusion

In conclusion, by studying two-photon resonant NFWM in Ba vapour with a coupling field we have observed that the linewidth of the four-wave mixing signal is proportional to the intensity of the coupling field. We have also given a comparison between the NFWM signal with a coupling field and the NFWM signal with beams of frequencies ω_1 and ω_3, demonstrating that the suppression of the signal is caused by atomic coherence induced by the coupling field. This method can be used as an effective spectroscopic tool to study atomic energy levels with several advantages. First, the phase matching conditions are not so stringent and can be achieved over a very wide frequency range. Second, this technique is Doppler-free when the incident lasers have narrow bandwidths, because if ω_1 is within the Doppler profile of the transition from $|0\rangle$ to $|1\rangle$, then only atoms in a specific velocity group will contribute to the signal. Third, due to the coherent radiation of signal and coupling field below saturation, we can study small transition dipoles. Most importantly, our method can measure the transition dipole moment between $|2\rangle$ and $|3\rangle$, which have such long radiative lifetimes that a direct detection of the fluorescence is difficult. Since $G_3 = \mu_3\varepsilon_3/\hbar$, μ_3 can be determined if the coupling field spot size and power are accurately measured. It also has the advantages of free choice of interaction volume, excellent spatial signal resolution and simple optical alignment.

References

[1] Sun J, Jiang Q, Mi X, Yu Z H and Fu P M 2004 *Acta Phys.Sin.* **53** 126 (in Chinese)

[2] Qu Z J, Liu S D and Yang C L 2005 *Acta Phys.Sin.* **54** 1156 (in Chinese)

[3] Liu X and Fang M F 2002 *Chin. Phys.* **11** 68

[4] Agarwal G S and Harshawardhan W 1996 *Phys. Rev. Lett.* **77** 1039

[5] Gao J Y, Yang S H, Wang D, Guo X Z, Chen K X, Jiang Y and Zhao B 2000 *Phys. Rev.* A **61** 023401

[6] Yan M, Rickey E G and Zhu Y F 2001 *Phys. Rev.* A **64** 043807

[7] Shakhmuratov R N, Rebane A, Mégret P and Odeurs J 2005 *Phys. Rev.* A **71** 053811

[8] Krmpot A, Mijailović M, Panić B, Lukić D, Kovačević A, Pantelić D and Jelenković B 2005 *Optics Express* **13** 1448

[9] Javan A, Javan A, Kocharovskaya O, Lee H and Scully M O 2002 *Phys. Rev.* A **66** 013805

[10] Mikhailov E E, Rostovtsev Y V and Welch G R 2002 *J. Mod. Opt.* **49** 2535

[11] Sun J, Zuo Z C, Mi X, Yu Z H, Jiang Q, Wang Y B, Wu L A and Fu P M 2004 *Phys. Rev.* A **70** 053820

[12] Sun J, Mi X, Yu Z H, Jiang Q, Zuo Z C, Wang Y B, Wu L A and Fu P M 2004 *Chin. Phys. Lett.* **21** 306

[13] Sun J, Zuo Z C, Mi X, Yu Z H, Wu L A and Fu P M 2005 *Acta Phys. Sin.* **54** 149 (in Chinese)

[14] Petch J C, Keitel C H, Knight P L and Marangos J P 1996 *Phys. Rev.* A **53** 543